Microchimica Acta (2020) 187:500
https://doi.org/10.1007/s00604-020-04475-5

ORIGINAL PAPER

A novel SWCNT-amplified "signal-on" electrochemical aptasensor for the determination of trace level of bisphenol A in human serum and lake water

Zhi Zhao[1,2] · Jun Zheng[3] · Emily P. Nguyen[4] · Dan Tao[1,2] · Jing Cheng[1,2] · Hongzhi Pan[5] · Ling Zhang[2] · Nicole Jaffrezic-Renault[6] · Zhenzhong Guo[1]

Received: 18 May 2020 / Accepted: 4 August 2020

Abstract

A novel "signal-on" electrochemical aptasensor was developed for ultrasensitive and specific detection of BPA, using single-walled carbon nanotubes (SWCNT) as the electro-catalytic probe for further signal amplification. The multi-walled carbon nanotubes (MWCNT), amino-functionalized magnetite, and gold nanoparticles (NH_2-Fe_3O_4/Au NPs) were applied first to modify the glassy carbon electrode (GCE) surface and to form a nanomaterial film with satisfactory conductive properties, stability, and biocompatibility. The BPA aptamer was then loaded onto the sensing platform by hybridization with complementary DNA (CDNA). In the presence of BPA it combines with the aptamer and the BPA-aptamer conjugate was released from the electrode;subsequently the added SWCNT and CDNA assembled quickly. Thus, the dual-amplification of the "signal-on" electrochemical aptasensor takes effect. The $[Fe(CN)_6]^{3-/4-}$ redox probe signal (ΔI) detected by DPV (differential pulse voltammetry) is proportional to the negative logarithm of BPA concentration between 10^{-19} M and 10^{-14} M. The detection limit is 0.08 aM. Importantly, the proposed biosensor represents a successful application for determination of BPA in human serum and lake water.

Keywords Bisphenol A · Aptasensor · Signal-on · Single-walled carbon nanotubes · Human serum · Lake water

Zhi Zhao and Jun Zheng contributed equally to this work.

Electronic supplementary material The online version of this article (https://doi.org/10.1007/s00604-020-04475-5) contains supplementary material, which is available to authorized users.

✉ Ling Zhang
zhangling@wust.edu.cn

✉ Nicole Jaffrezic-Renault
nicole.jaffrezic@univ-lyon1.fr

✉ Zhenzhong Guo
zhongbujueqi@hotmail.com

[1] Hubei Province Key Laboratory of Occupational Hazard Identification and Control, Wuhan University of Science and Technology, Wuhan 430065, People's Republic of China

[2] School of Public Health, Medical College, Wuhan University of Science and Technology, Wuhan 430065, People's Republic of China

[3] General Surgery Department, The Fifth Hospital of Wuhan, Wuhan 430050, People's Republic of China

[4] Nanobioelectronics & Biosensors Group, Catalan Institute of Nanoscience and Nanotechnology (ICN2), CSIC and BIST, Campus UAB, Bellaterra, 08193 Barcelona, Spain

[5] Collaborative Research Center, Shanghai University of Medicine and Health Sciences, Pudong, Shanghai, People's Republic of China

[6] Institute of Analytical Sciences, UMR-CNRS 5280, University of Lyon, 5, La Doua Street, 69100 Villeurbanne, France

Published online: 16 August 2020

Introduction

Recently, extensive studies show the possible health risks formed by endocrine-disrupting chemicals (EDCs), which are the exogenous agents that can interfere with the endocrine system by mimicking natural hormones or by blocking their metabolic pathways through environmental or developmental exposures [1]. Of the EDCs, bisphenol A (BPA) has been extensively utilized in the manufacturing of polycarbonate (PC) polymers, epoxy resins, and food storage since it was first synthesized and reported between the 1890s and early 1900s [2]. Researches stated that there are several diseases related to BPA exposure, such as obesity, diabetes, cardiovascular system disease, human neurological disorders, and hormone-sensitive female cancers [3]. Moreover, through real samples analysis more than 90% of people were found to have suffered the harm of BPA exposure [4]. It was shown that BPA is able to cause adverse health outcomes in as low concentrations as 4.4×10^{-12} mol L^{-1} and below [5]. Currently, various methods have been proposed to evaluate BPA levels in aqueous samples because the aquatic environment is the primary route for disposal of industrial waste [6]. Due to complex matrix influences of the biological materials, human internal fluids samples are more challenging for BPA detection when compared with aqueous samples [7]. In addition, it is reported blood levels of non-conjugated BPA are close to the actual BPA level of human exposure in the environment [8]. Hence, for BPA detection, developing analytic tools aiming at trace level detection in human body fluids and ordinary aqueous samples is urgent for ensuring human health.

Conventional methods for detection of BPA are based on large-scale instruments, including high-pressure liquid chromatography (HPLC) [9], liquid chromatography (LC) [10], and gas chromatography coupled with mass spectrometry (GC–MS) [11]. These methods can perform higher accuracy and stability. However, since the demands of high costs, complicated sample preparation, and professionally trained operators, these chromatography and mass spectrometry-based techniques may not be suitable for rapid and on-site determination of BPA in complex real samples [12]. The high selectivity and low detection limit are also critical in real samples detection. In this overall scenario, electrochemical methods have become excellent alternative analytical techniques for BPA rapid detection owing to their low detection limit, portability, cost effectiveness, and capability of real sample analysis [13]. As a result, they present the potential for efficiently evaluating the trace of BPA in human body fluids.

Aptamers are nucleic acid molecules which could specifically bond to proteins or other small molecules via folding into intricate 3D configurations. Aptamers, compared with antibodies and other affinity reagents, are easier to mass produce, have fewer immune responses, are smaller in size, have the ability to refold into the functional state, and can be engineered into aptasensors with simplicity [14]. In this regard, aptamers have the advantages as bio-recognition element for biosensors design because of the superior characteristics. Hence, extensive aptasensors have been developed by combining aptamer and other techniques, such as fluorescent aptasensors [15], electrochemiluminescence aptasensors [16], and photoelectrochemical aptasensors [17]. Owing to the fast responsiveness, low cost, and high affinity, electrochemical aptasensors have attracted considerable interests from many researchers. At the same time, one BPA molecule can only be trapped by one aptamer, evading the non-reversible polymerization of BPA, influencing the redox cycles on the surface of electrode [18].

Currently, signal switching and signal amplification are the dominant topics in electrochemical bio-sensing. Initially, signal switching was confined to fluorescence, where typically, a specific probe can turn off or turn on the signal upon recognition of the target. As some of the aptamers could trigger conformational changes when they bind to the target, this concept can be used to develop novel sensing schemes, thus, the introduction of electrochemical aptasensors. The signal switch could rely on the "signal-on" or "signal-off" scheme depending on the signal increase or decrease. Unfortunately, the aptasensors based on "signal-off" scheme may limit the sensitivity or produce a "false positive" result. The reported "signal-on" schemes [19, 20] for BPA detection are few, and there are still several limitations, like low sensitivity, elaborate preparation of probe (methylene blue/ferrocene-labeled DNA), and instability of the enzyme. Strategies to transform the interactions between aptamer and target into detectable signals and to develop more efficient "signal-on" electrochemical aptasensors remain still to be a fundamental problem.

For signal amplification, nanomaterials (NPs) are usually utilized to enhance the detectable signals by influencing the redox process. Gold nanoparticles (Au NPs) are excellent candidates as carriers for constructing sensing platform because of their excellent conductivity, strong antioxidant properties, and good biocompatibility. Thiolated compounds can bond through Au-S interactions easily [21]. Magnetite (Fe_3O_4) is the most commonly used magnetic NPs, it has good biocompatibility, non-genotoxicity, and can be easily prepared, to act as a scaffold for immobilization of biomolecules, such as enzymes [22]. Its high surface energy and large surface area allow electrons to transfer from the redox probe to electrode interface more efficiently. NH_2-functionalized Fe_3O_4 NPs (NH_2-Fe_3O_4 NPs) are capable of presenting multi-available bonding sites for other NPs bearing amido or carboxyl groups through covalent linkage, resulting in the improvement of the electrical activity [7]. Carbon nanotubes (CNT), divided into multi-walled carbon nanotubes (MWCNT) and single-walled carbon nanotubes (SWCNT) according to the layers of the graphene sheets, are hollow nanoscale cylinders made of carbon atoms. MWCNT have exhibited satisfactory electric

properties: large surface areas, strong π-π interactions between the graphene sheets, prominent mechanical strength, remarkable electrical conductivity, and stability [23]. Additionally, readily soluble functionalized MWCNT with carboxyl groups can bind the materials with other functional groups via covalent bonding such as amido bond, meanwhile enhancing the electrochemical signal. Besides owning outstanding conductivity, SWCNT could efficiently couple to single-stranded DNA (ssDNA), while rarely to double-stranded DNA (dsDNA) [24].

Inspired by the above content, we designed an electrochemical aptasensor in "signal-on" sensing scheme for BPA detection with high sensitivity, using SWCNT as the electrocatalytic probe on the glassy carbon electrode (GCE). Firstly, the GCE was modified by MWCNT and NH_2-functionalized Fe_3O_4/gold nanoparticles (NH_2-Fe_3O_4/Au NPs) to form a high conductive film. After the electrode interface was catalyzed by N1-((ethylimino) methylene)-N3 (EDC) and N-hydroxysuccinimide (NHS), the attachment of complementary 3′-NH_2-functionalized-DNA (CDNA) on the decorated electrode was consolidated via strong covalent amide bonding to the carboxyl groups on the surface of MWCNT. The BPA aptamer was then loaded onto the sensing platform by hybridization with the CDNA. In the presence of BPA, the BPA-aptamer conjugate is formed and released from the electrode. When adding the SWCNT on the electrode, SWCNT and CDNA-modified electrode assembled easily, resulting in the "signal-on" current of the platform. The excellent properties of the NPs and SWCNT contributed to the twice signal enhancement. The electrochemical performance varied significantly with and without the presence of BPA and was evaluated via differential pulse voltammetry (DPV) technology on the $[Fe(CN)_6]^{3-/4-}$ redox probe. This is the first amplification role of SWCNT as the electro-catalytic probe in "signal-on" electrochemical aptasensors for BPA trace detection. By combining the advantages of electrode modification and the specialty of SWCNT, the proposed "signal-on" scheme assures label-free, simple, efficient, and ultrasensitive detection of BPA.

Materials and methods

Materials

Sangon Biotechnology Co. (Shanghai, China) provided the synthesized and purified DNA strands, of which the sequences are given below [25]:

BPA aptamer: 5′-SH-CCG GTG GGT GGT CAG GTG GGA TAG CGT TCC GCG TAT GGC CCA GCG CAT CAC GGG TTC GCA CCA-3′. Complementary DNA (CDNA): 5′-TGG TGC GAA CCC GTG ATG CGC TGG GCC ATA-NH_2-3′. The information of other materials is presented in the Electronic Supporting Material.

Apparatus

CHI 660E electrochemical workstation (Shanghai Chenhua Instruments, China) was used for cyclic voltammetry (CV), current–time curve (I–t), and electrochemical impedance spectroscopy (EIS). DPVs were recorded by using a CS2350H biopotentiostat (Wuhan Corrtest Instruments, China). All electrochemical experiments were conducted by a traditional three-electrode arrangement. CVs were recorded in 5 mL $K_3Fe(CN)_6$/$K_4Fe(CN)_6$ (10 mM) solution containing 0.1 M PBS by sweeping potential from − 0.2 to 0.65 V at 0.1 Vs^{-1}. The I–t parameters were at the − 0.2 V initial potential lasting 400 s. EIS was performed with frequency scanning between 0.1 and 100,000 Hz in 5 mL $K_3Fe(CN)_6$/$K_4Fe(CN)_6$ (10 mM) solution containing 0.1 M PBS. The DPV parameters were the potential range: 0.8 to − 0.4 V, the amplitude: 0.05 V, the pulse width: 0.05 s, and pulse period: 2 s.

Electrode treatment

Electrostatic adsorption, electrodeposition, and covalent bonding are utilized to obtain the Apt-CDNA-modified electrodes according to the process shown in Scheme 1. The detailed procedures are provided in the Electronic Supporting Material.

Electrochemical measurement of detecting BPA

The Apt-CDNA-modified electrodes were incubated with 6 μL of BPA of various concentrations (10^{-19} M, 10^{-18} M, 10^{-17} M, 10^{-16} M, 10^{-15} M, 10^{-14} M) in 0.1 M PBS (pH = 7.4) for 30 min, then rinsed with 0.1 M PBS buffer. Next, 6 μL SWCNT (350 μg L^{-1}) was placed on the electrodes. After incubating for 1 h, 0.1 M PBS buffer was used to wash the electrodes' surface. The electrochemical signals were detected by DPV in 5 mL $K_3Fe(CN)_6$/$K_4Fe(CN)_6$ (10 mM) solution containing 0.1 M PBS.

Real samples preparation for detecting BPA

Human serum samples were obtained from healthy volunteers from Hubei community. Informed consents were received from all the volunteers. More details are presented in the Electronic Supporting Material. Increasing concentrations of BPA (10^{-19} M, 10^{-18} M, 10^{-17} M, 10^{-16} M, 10^{-15} M, 10^{-14} M) were spiked into human serum that was diluted 4000 times and the DPVs of each BPA concentration were recorded. Lake water samples were obtained from Qin Lake (Wuhan, China). Before analysis, all lake water samples were filtered through a 0.22-μm drainage membrane to remove the insoluble materials. All analytical processes were identical to that mentioned above.

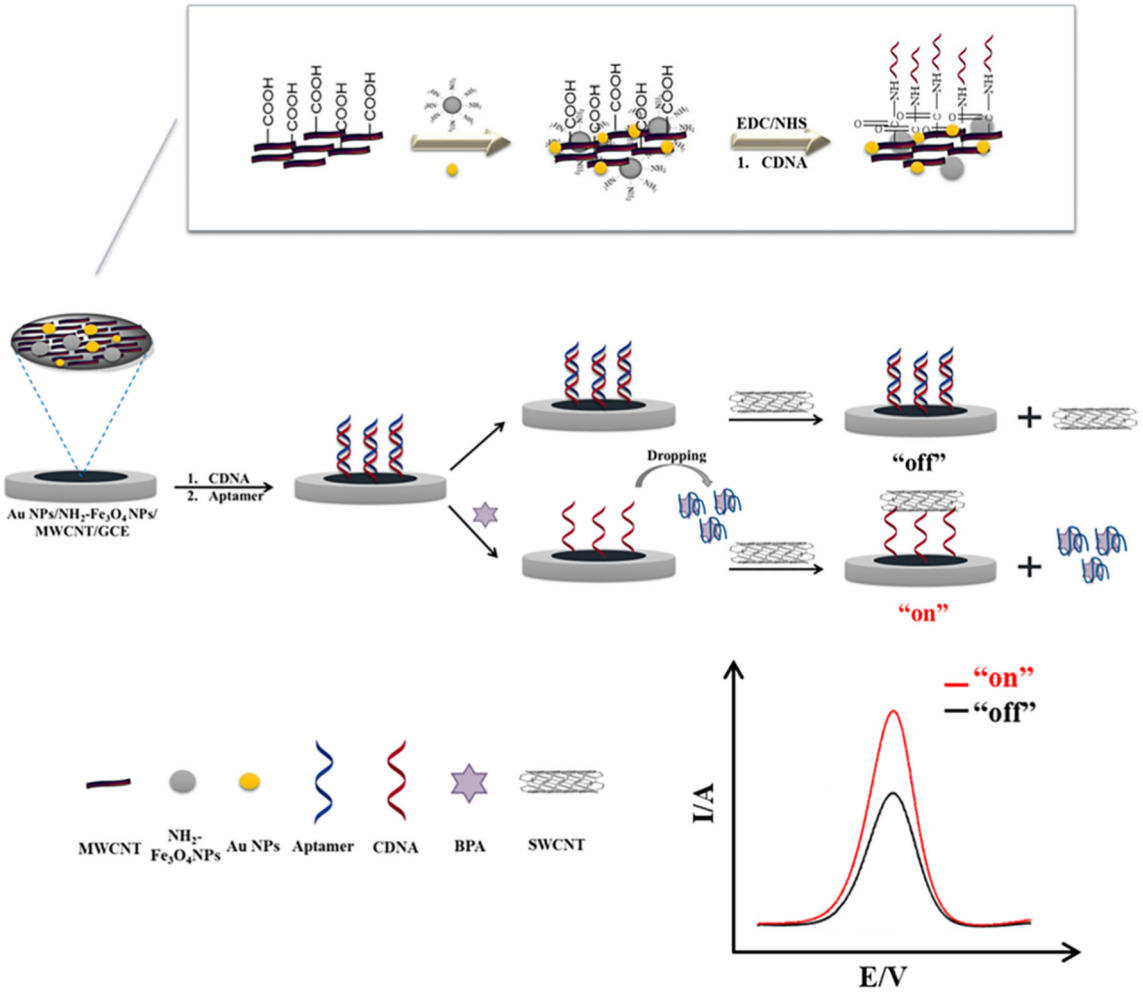

Scheme 1 Schematic diagram of fabricating a "signal-on" sensing model

Results and discussion

Sensing scheme

The mechanism of the proposed electrochemical aptasensor was designed based on a "signal-on" sensing scheme, which was made up of the fabrication of the GCE, MWCNT, NH_2-Fe_3O_4, Au NPs as the enhancers of electrochemical signal, and single-walled carbon nanotubes (SWCNT) as electrocatalytic probe that forms the ssDNA-SWCNT complex in the presence of BPA. This complex formation is not triggered in the absence of BPA.

The sensing strategy is depicted in Scheme 1. When there is no BPA, the dsDNA of aptamers and CDNA remain on the modified electrode. It has been demonstrated that SWCNT can bond to ssDNA rather than the hybridized strands. Only a small amount of SWCNT can bond to Apt-CDNA-modified GCE, resulting in a tiny current. In the presence of BPA, the binding capacity between the aptamers and their targets is stronger than the one between aptamers and their CDNA [26]. Thus, adding BPA could cause aptamer-target conjugation and the aptamer-target complex is released from the surface of the electrode, leaving the CDNA immobilized on modified electrode. At the moment, abundant SWCNT can bond to CDNA through π-π interactions [27], thereby the complex formation forms, which means the SWCNT could amplify the electrochemical signal further besides already traditional amplification relying on electrode modification directly. Because of the change of conformation and the enhancement of the electron transport between the redox probe and electrode interface, the "signal-on" electrochemical signal upsurges comparatively.

Morphology and structure characterization

Figure 1 shows the morphology features of the MWCNT, NH_2-Fe_3O_4, and SWCNT through transmission electron microscope (TEM) images. From Fig. 1(a), it could be seen that the MWCNT has a hollow tubular structure crisscrossed in the solution, with average in outer diameters of 15 nm and 5 nm for the inner diameters, and length in the range of micrometers, which is helpful for forming a porous netlike film. The

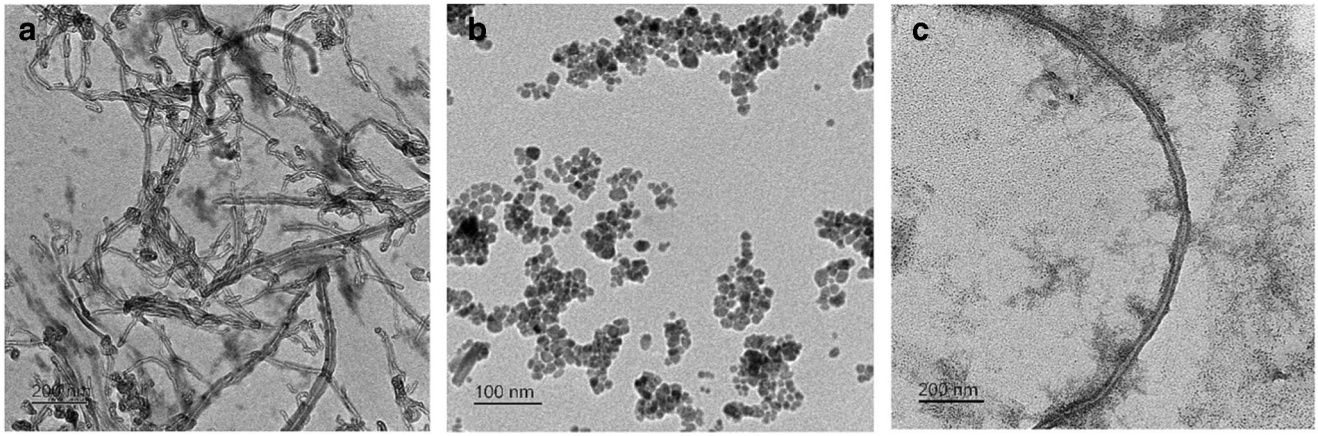

Fig. 1 TEM images of the MWCNT (**a**), NH_2-Fe_3O_4 NPs (**b**), and SWCNT (**c**)

representative TEM image of NH_2-Fe_3O_4 NPs displays spheroidal particle with a diameter of 8–10 nm (Fig. 1(b)). Therefore, the NH_2-Fe_3O_4 NPs fixing onto the MWCNT/GCE is promising, resulting in a large surface area and improving the electron-transfer kinetics. The SWCNT TEM image (Fig. 1(c)) is similar with MWCNT's TEM image, both presenting a hollow tubular structure. Fourier infrared spectrums (FT-IR) and scanning electron microscope (SEM) image were also utilized for the characterization of nanomaterials and electrode modification as Fig. S1 ~ Fig. S3 show.

The fabrication of the "signal-on" sensing platform plays a critical part in the response of the electrochemical aptasensor. EIS is an alternative, commonly used tool for investigating the change in the electrode modification procedure. In the EIS Nyquist plot, the semicircle part, at higher frequencies, relates to the charge-transfer limited procedure. If the diameter of semicircle increases, the interfacial charge-transfer resistance (Rct) increases correspondingly. The general inset circuit is for fitting the impedance data of the fabrication process, including three portions: Rs represents electrolyte resistance, CPE represents the constant phase element, Ret represents the electron-transfer resistance, and Ws represents the Warburg impedance [28]. Figure 2(a) shows the bare electrode (curve a) had a relatively small semicircle diameter, revealing the bare electrode was clean thoroughly as the electron transfer was rapid. Curve b suggests that the Rct of the MWCNT/GCE shrank slightly comparing with that of the bare GCE, which indicated MWCNT enhanced the conductivity of the electrode. The modification of the electrode with NH_2-Fe_3O_4/Au NPs caused a reduction in the Rct (curve c), which is understandable because the Au NPs and NH_2-Fe_3O_4 NPs fixed on the MWCNT/GCE have satisfactory large surface area, which can facilitate the electron transport kinetics of $[Fe(CN)_6]^{3-/4-}$ on the electrode surface. Furthermore, Rct increased upon the addition of CDNA on the Au NPs/NH_2-Fe_3O_4/MWCNT/GCE (curve d), demonstrating the

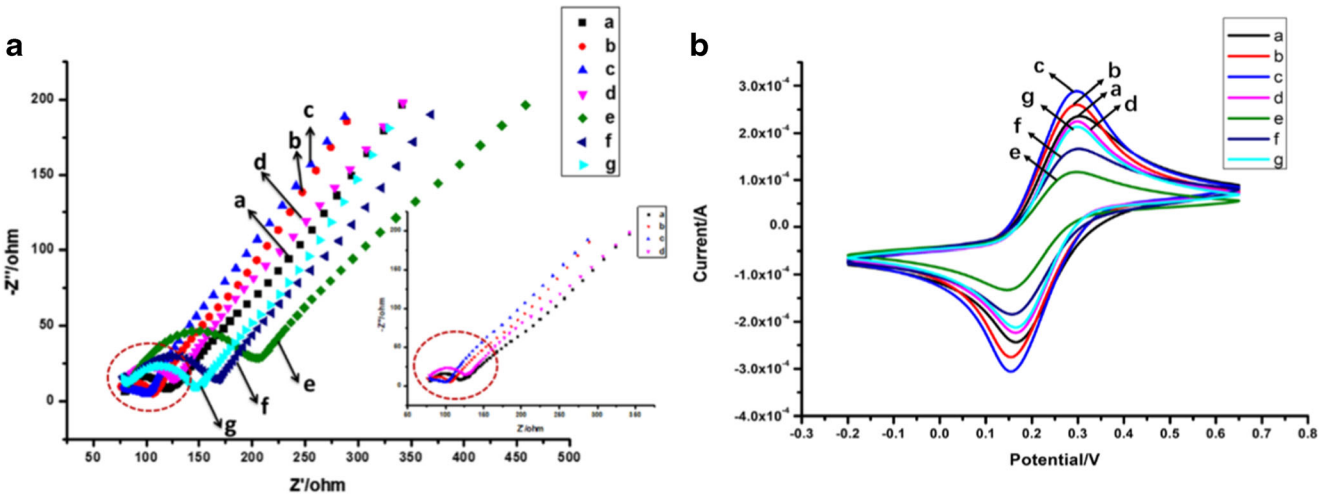

Fig. 2 Proof of fabricating the electrochemical aptasensor. Electrochemical impedance spectroscopy (**a**) and cyclic voltammetry (**b**) responses for bare GCE (a), MWCNT/GCE (b), Au NPs/NH_2-Fe_3O_4/MWCNT/GCE (c), CDNA/Au NPs/NH_2-Fe_3O_4/MWCNT/GCE (d), aptamer/CDNA/Au NPs/NH_2-Fe_3O_4/MWCNT/GCE (e), SWCNT + aptamer/CDNA/Au NPs/NH_2-Fe_3O_4/MWCNT/GCE (f), and BPA + SWCNT + aptamer/CDNA/Au NPs/NH_2-Fe_3O_4/MWCNT/GCE (g) recorded at 10 mM $K_4Fe(CN)_6/K_3Fe(CN)_6$ (1: 1) in 0.1 M PBS (pH = 7.4)

attachment of CDNA on the modified electrode. Since CDNA has a large number of negatively charged phosphate groups, and the redox probe is also negatively charged, the CDNA will repel the active probe on the electrode surface, greatly hindering the electron transport. After incubating the BPA aptamer with CDNA-modified electrode, the Rct (curve e) further increased owing to the hybridization between the CDNA and aptamer which has more negatively charged phosphate group. Upon incubating the SWCNT on the Apt-CDNA-modified electrode, although the "signal-on" complex formation could not come into being, the Rct (curve f) decreased, owing to the excellent electrochemical properties of little SWCNT which interacts with dsDNA. In the presence of BPA, the Rct (curve g) decreased significantly and even approached the Rct of Au NPs/NH_2-Fe_3O_4/MWCNT/GCE. This can be attributed to the formation of the aptamer-target conjugates and following ssDNA-SWCNT complex. As hypothesized, the "signal-on" sensing scheme took effect.

CV measurements were conducted to further confirm the construction of the "signal-on" sensing platform. Presented in Fig. 2(b) is the peak current that shows an increase when the bare GCE was decorated (curve a) with MWCNT (curve b) and NH_2-Fe_3O_4/Au NPs (curve c). This change can be attributed to the outstanding signal-amplification ability of the NPs. Grafting of the CDNA at the surface of Au NPs/NH_2-Fe_3O_4/MWCNT/GCE resulted in a decrease of both the anodic peak and cathodic peak currents (curve d), indicating the electrostatic repulsion of the large amount of negatively charged phosphate groups blocking the electron of probe to the surface. Upon the immobilization of aptamer, the peak current (curve e) decreased further, verifying the loading of aptamer on the CDNA-modified electrode via hybridizing with CDNA. After incubating SWCNT with Apt-CDNA-modified electrode for 1 h, as the SWCNTs could amplify the electrochemical signal, the peak current (curve f) enhanced slightly. In the presence of BPA, due to the "signal-on" strategy, the electrochemical signal (curve g) improved significantly, verifying the strong interaction between SWCNT and CDNA in the "signal-on" sensing scheme. Results of CVs and EIS are equivalent to each other and the experimental data above reveal the "signal-on" sensing platform has been established successfully.

Optimizing the experimental parameters

To evaluate the performance characteristics of the biosensor, the conditions influencing the capability of the aptasensor were optimized. Figure 3(a) shows the effect of the incubation time for BPA on the Apt-CDNA-modified electrode. After incubation with the modified electrode, the value of peak current ΔI (I_P-I_0, I_P: peak current in presence, I_0: peak current when there is no BPA) was obtained from the DPVs for assessing the incubation impact on the aptasensor behavior. The response of the current significantly increased with the incubation time and plateaued at 30 min due to the gradual saturation of the binding sites by the BPA. Therefore, for the Apt-CDNA-modified electrode reacting with BPA, 30 min was chosen as the appropriate incubation time.

Figure 3(b) shows the effect of the dilution ratio for human serum. The BPA solutions diluted by human serum were incubated with the Apt-CDNA-modified electrode. The DPVs were then recorded to estimate the influence of the dilution ratio. The peak current I_P decreased significantly as the serum dilution ratio increased from 1:500 to 1:4000 and increased slightly as the serum dilution ratio increased from 1:4000 to 1:5000. Considering the minimum amount of matrix effects from the human serum for the current responses and the errors from practical limit on serial dilution, 1:4000 was the optimal dilution ratio. Similarly, the effect of the dilution ratio of the lake water was assessed and the results suggested that all the lake water samples were to be diluted 4000 times when preparing the concentration range of BPA solutions.

In addition, the effect of the amount of the modification materials and the concentration of aptamer were investigated

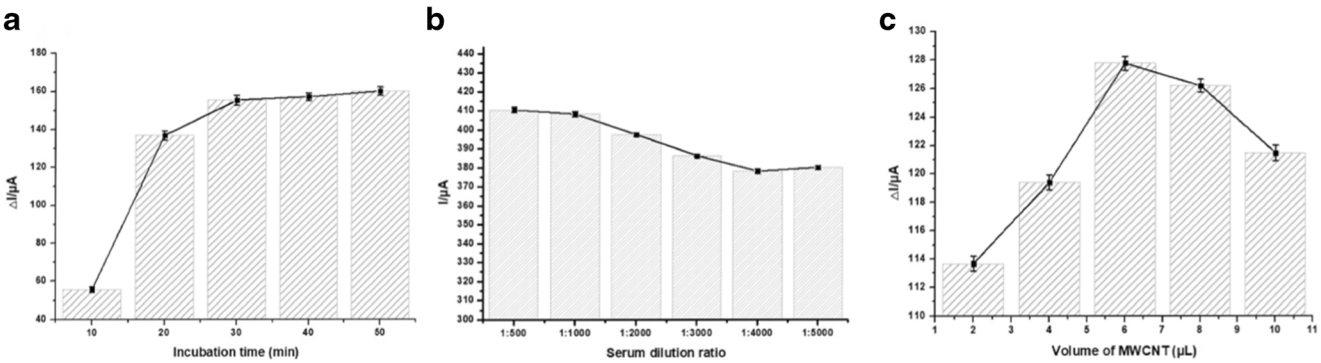

Fig. 3 Optimization of the experimental parameters: incubation time (**a**) in presence of 10^{-17} M of BPA in 0.1 M PBS (pH = 7.4), serum dilution ratio (**b**) in presence of 10^{-17} M of BPA in diluted human serum, and volume of MWCNT (**c**) in presence of 10^{-17} M of BPA in 0.1 M PBS (pH = 7.4)

by recording the DPVs against the same concentration of BPA. The volume of the modification materials influences the thickness of the film formed on the electrode surface, which affects the transport rate of electrons. For MWCNT, it is worth noting that the peak value of the current response appeared at 6 μL (Fig. 3(c)). Larger MWCNT volume results in thicker MWCNT films, which would induce electron-transfer hindrance, active site blockage, and decrease the efficiency of CDNA immobilization, while smaller volume of MWCNT cannot fully cover electrode surface and negate the role of the MWCNT for signal amplification. Hence, the best dropping volume of the MWCNT was 6 μL. The optimal modifying volume of the NH_2-Fe_3O_4 NPs was selected as 6 μL, similarly. Accordingly, the optimized concentration of aptamer was also explored to be 20 μM as Fig. S4 displays.

Quantitative BPA detecting

Under the above optimal experimental conditions, the DPV signal of the $[Fe(CN)_6]^{3-/4-}$ redox probe was used for detecting the trace amount of BPA in range of 10^{-19} M to 10^{-14} M. In the presence of BPA, owing to the formation of the BPA-aptamer conjugation, the symbolizing "signal-on" cage conformation which was made of CDNA-modified electrode and SWCNT could be triggered. Hence, when there are more BPA in the solution, more aptamer would release from the modified electrode to conjugate with BPA, accordingly, on the electrode, more dsDNA: CDNA are presented for interacting with SWCNT, and the electrochemical signal could be amplified further and better.

Figure 4(a) shows that the peak current increased gradually when the BPA concentration increased, validating the above

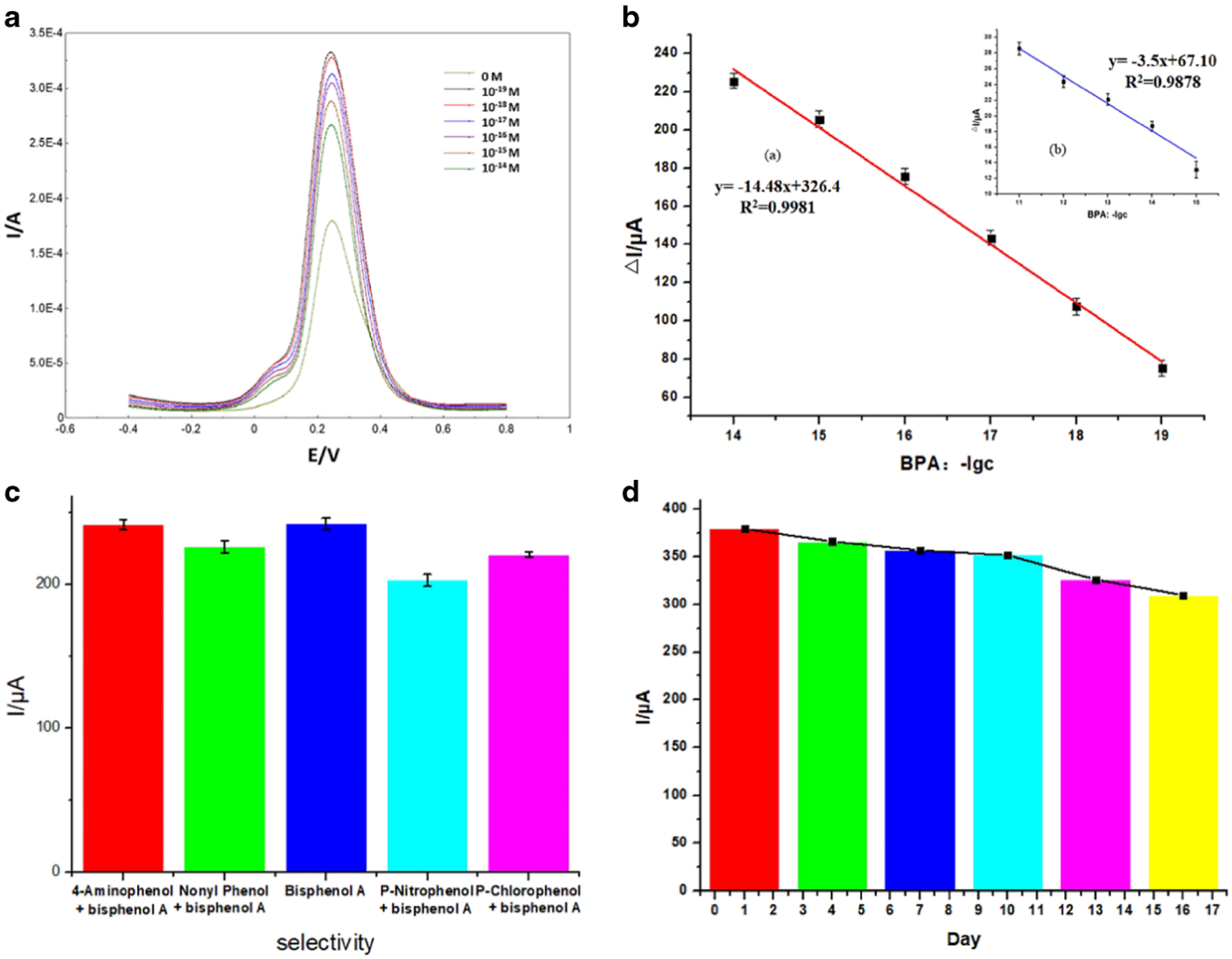

Fig. 4 (**a**) Differential pulse voltammetry responses at different concentrations of BPA (10^{-19} M, 10^{-18} M, 10^{-17} M, 10^{-16} M, 10^{-15} M, 10^{-14} M). (**b**) The calibration curves, (a) the Apt-CDNA-modified electrode, and (b) the Apt-modified electrode of the ΔI value and the negative logarithm of BPA concentration. The inset shows the calibration plot of Apt-modified electrode detecting different concentrations of BPA (10^{-15} M, 10^{-14} M, 10^{-13} M, 10^{-12} M, 10^{-11} M) directly. (**c**) Target selectivity of the developed electrochemical aptasensor. (**d**) The stability of the developed electrochemical aptasensor for a long-term storage at 4 °C

mechanism. The resulting standard curve (curve a, Fig. 4(b)) exhibits that the variation of peak current ΔI is linearly dependent on the negative logarithm of BPA concentration ranging from 10^{-19} M to 10^{-14} M with a correlation coefficient (R^2) of 0.9981. According to the International Union of Pure and Applied Chemistry (IUPAC) [29], the limit of detection (LOD) is set as 3 times the standard deviation of blank/slope and was found to be 0.08 aM. It follows that the electrochemical aptasensor based on the "signal-on" sensing scheme presents an ultra-higher sensitivity than most previously reported electrochemical sensors and other transducing methods for BPA detection, as reported in Table S1. Relative standard deviations (RSD) for different BPA concentrations (10^{-19} M, 10^{-18} M, 10^{-17} M, 10^{-16} M, 10^{-15} M, 10^{-14} M) were 2.1%, 1.9%, 2.2%, 2.3%, 2.0%, and 2.2% (all less than 5%), respectively.

In addition, to further demonstrate the dual-signal amplification superiority of the "signal-on" sensing scheme and the performance of the electrochemical aptasensor, control experiments were conducted by utilizing the Au NPs/NH_2-Fe_3O_4/MWCNT-based aptamer sensor for tracing BPA. Linear dependence (curve b, Fig. 4(b)) was observed at concentration ranges of 10^{-15} M to 10^{-11} M, with a correlation coefficient of 0.9878. The LOD was 0.75 fM according to the similar calculating process. It can be seen that the SWCNT-amplified "signal-on" electrochemical aptasensor using single-walled carbon nanotubes (SWCNT) as electrocatalytic probe presents lower LOD and higher sensitivity, which can be attributed to the two amplification features: (i) The various modified NPs could produce a synergic effect such as conductivity, electrochemical activity, and compatibility; the electron transduction could be improved, resulting in lower LOD [30]. Therefore, the Au NPs/NH_2-Fe_3O_4/MWCNT nanocomposite was able to enhance the individual characteristics of every nanomaterial, and further facilitate the property of electron transfer eventually. (ii) The core part: the SWCNT was as electro-catalytic probe. In the general conditions, decreasing the LOD relies on the amplification of

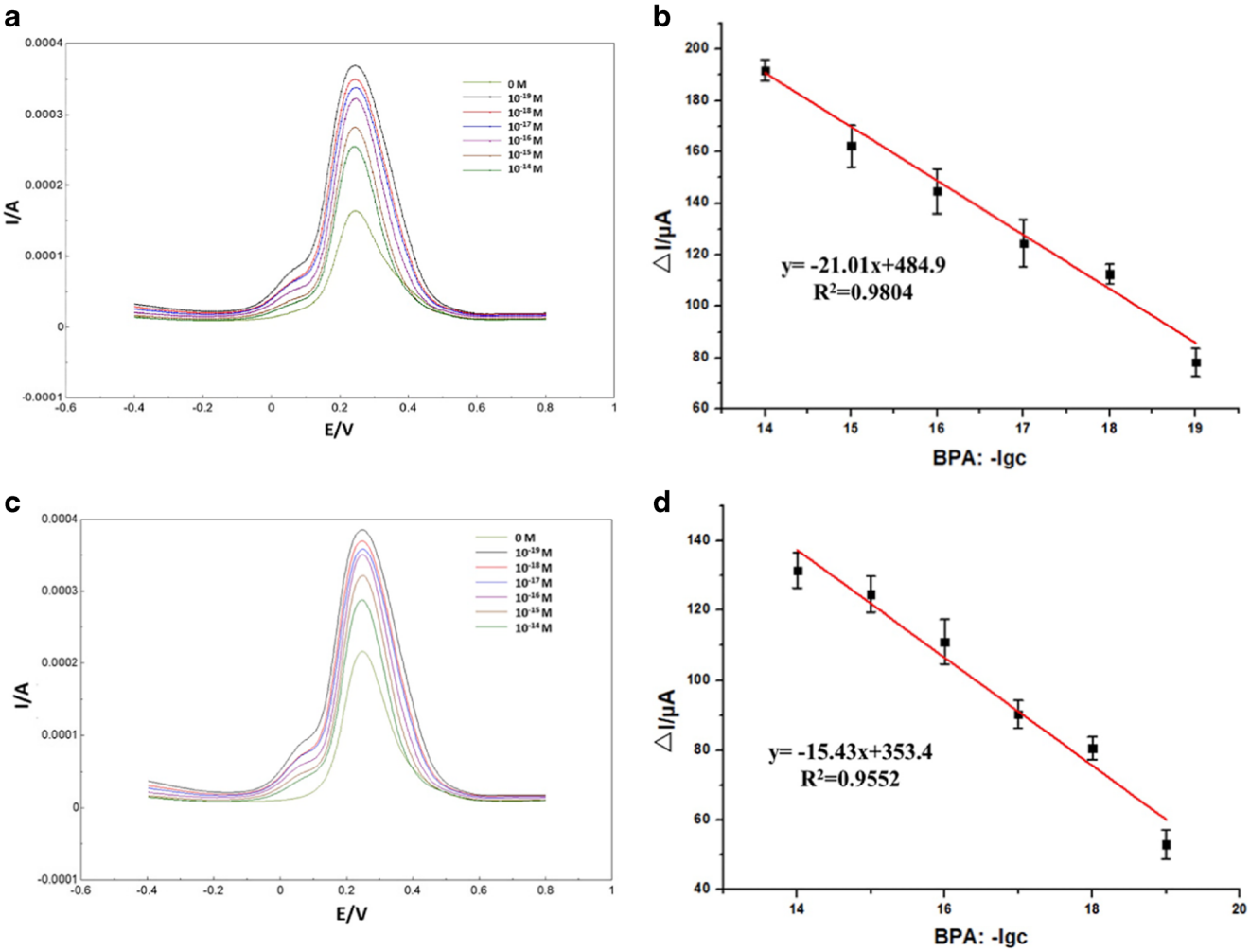

Fig. 5 (**a**) Differential pulse voltammetry responses at different concentrations of BPA (10^{-19} M, 10^{-18} M, 10^{-17} M, 10^{-16} M, 10^{-15} M, 10^{-14} M) in human serum. (**b**) BPA calibration curve in human serum. (**c**) Differential pulse voltammetry responses at different concentrations of BPA (10^{-19} M, 10^{-18} M, 10^{-17} M, 10^{-16} M, 10^{-15} M, 10^{-14} M) in lake water. (**d**) BPA calibration curve in lake water

Table 1 Determination and recoveries of BPA in human serum transferred from different human serum samples ($n = 3$) and lake water collected from different lake water samples ($n = 3$)

Sample	Added concentration	Found	Recoveries (%)	RSD (%)
Human serum	0.50 aM	0.52 aM	103.24	2.20
	50.00 aM	50.90 aM	101.81	3.68
	5.00 fM	4.98 fM	99.69	1.60
Lake water	0.50 aM	0.49 aM	98.23	3.16
	50.00 aM	49.09 aM	98.17	3.97
	5.00 fM	4.94 fM	98.84	3.18

original signal, like the modification of the NPs. However, in most aptasensor designs, after the attachment of the aptamer, it is often difficult to modify the NPs on the electrode, which can influence the activity of the aptamer directly. The introduction of the "signal-on" switching scheme skillfully solves the problem by taking advantages of the specific cooperation between SWCNT and CDNA. In the presence of BPA, the complex formation made of SWCNT and CDNA is triggered, whose amount increases as the concentration increases. The design cleverly reuses the outstanding signal-amplifying merits of the SWCNT without destroying the aptamer recognition property for the target molecules. This is the essential reason why the "signal-on" sensing scheme could work.

Specificity, stability, and reproducibility of the electrochemical aptasensor

Specificity plays a considerable role in confirming the practicability of analytical methods. The DPV current responses of the biosensor were recorded toward 10^{-15} M BPA and 10^{-12} M 4-aminophenol, 10^{-15} M BPA and 10^{-12} M nonyl phenol, 10^{-15} M BPA, 10^{-15} M BPA and 10^{-12} M p-nitrophenol, and 10^{-15} M BPA and 10^{-12} M p-chlorophenol. Figure 4(c) shows that in the presence of 4-aminophenol, nonyl phenol, p-nitrophenol, and p-chlorophenol, the peak current is close to that of the BPA alone, with a different value of less than 3%. Such a reasonable specificity of the electrochemical aptasensor for detecting BPA is due to the prominent selectivity of the aptamer. Besides, the electrochemical responses were caused by the conformational change on the electrode, not the electroactive substances, which frequently appear as disruptors in the real samples. Thus, the designed aptasensor presents high selectivity.

To examine the long-term stability of the biosensor, the sensors were stored at 4 °C and the DPV current responses of the sensor were evaluated toward the same concentration of BPA every 3 days. The aptasensors reserved 96.5% of its initial value after three days storage, 92.6% after 10 days, and 81.5% after 16 days (Fig. 4(d)), this indicating the good stability of the aptasensors. Besides, the reproducibility of the proposed aptasensor has been displayed in Fig. S5. These results suggest the proposed electrochemical aptasensor has excellent selectivity, stability, and reproducibility.

Real sample measurement

To estimate the function of the developed aptasensor with real samples, the constructed aptasensors were implemented for measuring BPA in human serum (Fig. 5(a), Fig. 5(b)) and lake water (Fig. 5(c), Fig. 5(d)). Being similar to the mechanism in the PBS, the peak current increased gradually when the BPA concentration increased. However, due to the matrix effect of human serum and the more complex solution environment compared with PBS, the fitting effect of the obtained standard curve was relatively not as good as that in PBS. The linear dependencies of spiked BPA analysis yielded an equation of $\Delta I\ (\mu A) = -21.01\ \lg c_{[BPA]} + 484.9$ with a correlation coefficient of 0.9804. The results of BPA recovery in human serum samples are presented in Table 1. The recoveries were between 99 and 104%. For lake water samples, as the data exhibit, the linear dependencies of the aptasensors response versus −lg of BPA concentration is fitted by the equation: $\Delta I\ (\mu A) = -15.43\ \lg c_{[BPA]} + 353.4$ with a correlation coefficient of 0.9552. The recoveries of BPA spiked lake water samples were in the range of 98–99% (Table 1). These results indicate that the constructed aptasensor could be applied for the detection of BPA in human serum and lake water. However, the electrochemical aptasensors cannot be reused for detection of BPA due to the fact the affinity constant between BPA and its aptamer is far higher than that of the aptamer and CDNA combining into dsDNA [19].

Conclusion

In brief, an electrochemical aptasensor was developed for ultrasensitive detection of BPA based on the modification of the GCE with the NPs: MWCNT, amino-functionalized Fe_3O_4 NPs and Au NPs, and the use of SWCNT as an electrocatalytic probe. This is the first reported "signal-on" electrochemical aptasensor utilized for BPA detection, further amplified by SWCNT. The LOD for BPA detection was calculated to be as low as 0.08 aM. The aptasensor also presented

remarkable specificity to BPA, long-term stability, and reproducibility. Furthermore, the biosensor is robust and can be applied to the reliable monitoring of spiked BPA in human serum and lake water samples with good recovery rates, suggesting the promising potential for clinical diagnosis and rapid environmental monitoring. The excellent performance of the aptasensor is attributed to the dual-signal amplification from NPs and CDNA-SWCNT cooperation. More importantly, the "signal-on" sensing scheme is modular and versatile, which can be easily extended to detect other EDCs by only replacing aptamers as the specific recognition elements.

Funding information This study was financially supported by the "ChuTian Scholar" Project Award, China; Hubei Province Introduction of Foreign Talents Project, China (No. 2); Foreign Expert Project of the Ministry of Science and Technology, China (No. G20190227002); National Natural Science Foundation of China (No. 81973097); and Excellent young and middle-aged scientific research and innovation team Fund, Wuhan University of Science and Technology (No. 2018TDZ03).

Compliance with ethical standards

Conflict of interest The authors declare that they have no competing interests.

References

1. Gugoasa LAD (2020) Review—electrochemical sensors for determination of the endocrine disruptor, bisphenol A. J Electrochem Soc 167:037506. https://doi.org/10.1149/2.0062003jes
2. Lim HJ, Chua B, Son A (2017) Detection of bisphenol A using palm-size NanoAptamer analyzer. Biosens Bioelectron 94:10–18. https://doi.org/10.1016/j.bios.2017.02.029
3. Jiang Y, Li J, Xu S, Zhou Y, Zhao H, Li Y, Xiong C, Sun X, Liu H, Liu W, Peng Y, Hu C, Cai Z, Xia W (2020) Prenatal exposure to bisphenol A and its alternatives and child neurodevelopment at 2 years. J Hazard Mater 388:121774. https://doi.org/10.1016/j.jhazmat.2019.121774
4. Mustieles V, Pérez-Lobato R, Olea N, Fernández MF (2015) Bisphenol A: human exposure and neurobehavior. NeuroToxicology 49:174–184
5. Erjavec B, Hudoklin P, Perc K, Tišler T, Dolenc MS, Pintar A (2016) Glass fiber-supported TiO2 photocatalyst: efficient mineralization and removal of toxicity/estrogenicity of bisphenol A and its analogs. Appl Catal B Environ 183:149–158. https://doi.org/10.1016/j.apcatb.2015.10.033
6. Moreman J, Lee O, Trznadel M, David A, Kudoh T, Tyler CR (2017) Acute toxicity, teratogenic, and estrogenic effects of bisphenol A and its alternative replacements bisphenol S, bisphenol F, and bisphenol AF in zebrafish embryo-larvae. Environ Sci Technol 51:12796–12805. https://doi.org/10.1021/acs.est.7b03283
7. Azadbakht A, Beirnvand S (2017) Voltammetric aptamer-based switch probes for sensing diclofenac using a glassy carbon electrode modified with a composite prepared from gold nanoparticles, carbon nanotubes and amino-functionalized Fe3O4 nanoparticles. Microchim Acta 184:2825–2835. https://doi.org/10.1007/s00604-017-2285-1
8. Azevedo LF, Hornos Carneiro MF, Dechandt CRP, Cassoli JS, Alberici LC, Barbosa F Jr (2020) Global liver proteomic analysis of Wistar rats chronically exposed to low-levels of bisphenol A and S. Environ Res 182:182. https://doi.org/10.1016/j.envres.2019.109080
9. Rozaini MNH, Yahaya N, Saad B et al (2017) Rapid ultrasound assisted emulsification micro-solid phase extraction based on molecularly imprinted polymer for HPLC-DAD determination of bisphenol A in aqueous matrices. Talanta 171:242–249. https://doi.org/10.1016/j.talanta.2017.05.006
10. Kolatorova Sosvorova L, Chlupacova T, Vitku J, Vlk M, Heracek J, Starka L, Saman D, Simkova M, Hampl R (2017) Determination of selected bisphenols, parabens and estrogens in human plasma using LC-MS/MS. Talanta 174:21–28. https://doi.org/10.1016/j.talanta.2017.05.070
11. Wang Q, Zhu L, Chen M, Ma X, Wang X, Xia J (2017) Simultaneously determination of bisphenol A and its alternatives in sediment by ultrasound-assisted and solid phase extractions followed by derivatization using GC-MS. Chemosphere 169:709–715. https://doi.org/10.1016/j.chemosphere.2016.11.095
12. Alam AU, Deen MJ (2020) Bisphenol A electrochemical sensor using graphene oxide and β-cyclodextrin-functionalized multiwalled carbon nanotubes. Anal Chem 92:5532–5539. https://doi.org/10.1021/acs.analchem.0c00402
13. Huang JY, Zhao L, Lei W, Wen W, Wang YJ, Bao T, Xiong HY, Zhang XH, Wang SF (2018) A high-sensitivity electrochemical aptasensor of carcinoembryonic antigen based on graphene quantum dots-ionic liquid-nafion nanomatrix and DNAzyme-assisted signal amplification strategy. Biosens Bioelectron 99:28–33. https://doi.org/10.1016/j.bios.2017.07.036
14. Dunn MR, Jimenez RM, Chaput JC (2017) Analysis of aptamer discovery and technology. Nat Rev Chem 1(10):0076. https://doi.org/10.1038/s41570-017-0076
15. Esmaelpourfarkhani M, Abnous K, Taghdisi SM, Chamsaz M (2020) A novel turn-off fluorescent aptasensor for ampicillin detection based on perylenetetracarboxylic acid diimide and gold nanoparticles. Biosens Bioelectron 164:164. https://doi.org/10.1016/j.bios.2020.112329
16. Muzyka K, Saqib M, Liu Z, Zhang W, Xu G (2017) Progress and challenges in electrochemiluminescent aptasensors. Biosens Bioelectron 92:241–258
17. Zhang Y, Hao N, Zhou Z, Hua R, Qian J, Liu Q, Li H, Wang K (2017) A potentiometric resolved ratiometric photoelectrochemical aptasensor. Chem Commun 53:5810–5813. https://doi.org/10.1039/c7cc01582h
18. Zhu Y, Zhou C, Yan X, Yan Y, Wang Q (2015) Aptamer-functionalized nanoporous gold film for high-performance direct electrochemical detection of bisphenol A in human serum. Anal Chim Acta 883:81–89. https://doi.org/10.1016/j.aca.2015.05.002
19. Yu P, Liu Y, Zhang X, Zhou J, Xiong E, Li X, Chen J (2016) A novel electrochemical aptasensor for bisphenol A assay based on triple-signaling strategy. Biosens Bioelectron 79:22–28. https://doi.org/10.1016/j.bios.2015.12.007
20. Rao H, Chen M, Ge H, Lu Z, Liu X, Zou P, Wang X, He H, Zeng X, Wang Y (2017) A novel electrochemical sensor based on Au@PANI composites film modified glassy carbon electrode binding molecular imprinting technique for the determination of melamine. Biosens Bioelectron 87:1029–1035. https://doi.org/10.1016/j.bios.2016.09.074
21. Peng D, Liang RP, Huang H, Qiu JD (2016) Electrochemical immunosensor for carcinoembryonic antigen based on signal amplification strategy of graphene and Fe3O4/Au NPs. J Electroanal Chem 761:112–117. https://doi.org/10.1016/j.jelechem.2015.12.014
22. Ran F, Zou Y, Xu Y et al (2019) Fe3O4@MoS2@PEI-facilitated enzyme tethering for efficient removal of persistent organic pollutants in water. Chem Eng J 375. https://doi.org/10.1016/j.cej.2019.121947

23. Ali MY, Alam AU, Howlader MMR (2020) Fabrication of highly sensitive bisphenol A electrochemical sensor amplified with chemically modified multiwall carbon nanotubes and β-cyclodextrin. Sensors Actuators B Chem 320. https://doi.org/10.1016/j.snb.2020.128319
24. Tian J, Zhao H, Liu M, Chen Y, Quan X (2012) Detection of influenza A virus based on fluorescence resonance energy transfer from quantum dots to carbon nanotubes. Anal Chim Acta 723:83–87. https://doi.org/10.1016/j.aca.2012.02.030
25. Ye S, Ye R, Shi Y, Qiu B, Guo L, Huang D, Lin Z, Chen G (2017) Highly sensitive aptamer based on electrochemiluminescence biosensor for label-free detection of bisphenol A. Anal Bioanal Chem 409:7145–7151. https://doi.org/10.1007/s00216-017-0673-3
26. Wu S, Zhang H, Shi Z, Duan N, Fang CC, Dai S, Wang Z (2015) Aptamer-based fluorescence biosensor for chloramphenicol determination using upconversion nanoparticles. Food Control 50:597–604. https://doi.org/10.1016/j.foodcont.2014.10.003
27. He Q, Wu Q, Feng X, Liao Z, Peng W, Liu Y, Peng D, Liu Z, Mo M (2020) Interfacing DNA with nanoparticles: surface science and its applications in biosensing. Int J Biol Macromol 151:757–780
28. Ashraf G, Asif M, Aziz A et al (2019) Nanocomposites consisting of copper and copper oxide incorporated into MoS4 nanostructures for sensitive voltammetric determination of bisphenol A. Microchim Acta 186. https://doi.org/10.1007/s00604-019-3406-9
29. Hernandez Hernandez F, Medina Escriche J (1984) Fluorimetric determination of aluminium with morin after extraction with isobutyl methyl ketone part I. Fluorescence of the aluminium - morin complex in an isobutyl methyl ketone - ethanol - water system. Analyst 109:1585–1588. https://doi.org/10.1039/AN9840901585
30. He H, Sun DW, Pu H, Huang L (2020) Bridging Fe3O4@Au nanoflowers and Au@Ag nanospheres with aptamer for ultrasensitive SERS detection of aflatoxin B1. Food Chem 324:126832. https://doi.org/10.1016/j.foodchem.2020.126832